Journal of
Engineering Sciences
Faculty of Engineering
Assiut University
JES
مجلة
العلوم الهندسية
كلية الهندسة
جامعة أسيوط
journal homepage: http://jesaun.journals.ekb.eg

Performance Based Seismic Assessment of Regular and Irregular Tube-in-Tube RC Structures Using Pushover Analysis

Received 17 July 2025; Revised 19 September 2025; Accepted 20 September 2025

Heba Salem *[1]
Hilal Hassan [2]
Mahmoud Abd El Hamid [3]
Wadid William [4]

Keywords
Seismic Evaluation
Tube-in-Tube
Pushover Analysis
Inter Story Drift

Abstract: Seismic activity remains a critical concern in the design of high-rise buildings due to their height and flexibility, which amplify lateral responses during earthquakes. Among various structural systems, the tube-in-tube configuration offers enhanced lateral stiffness and energy dissipation capacity, making it a widely adopted solution for tall structures in seismic regions. This study evaluates the seismic performance of reinforced concrete tube-in-tube buildings using nonlinear static pushover analysis. Three building heights (G+29), (G+39), and (G+49) stories were analyzed under seismic zones 2, 4 and 5b based on the Egyptian Code (ECP-201) for loading and the ATC-40 guidelines for performance evaluation. Both regular and vertically irregular configurations were modeled using SeismoStruct software. The analysis applied the Displacement Coefficient Method (DCM) to estimate inelastic demands, assessing inter-story drift ratios, target displacements, and plastic hinge distributions. The results revealed that geometric irregularities significantly increase lateral displacements and hinge concentration, especially in higher seismic zones. Performance levels were evaluated using plastic hinge criteria and pushover curves. Retrofitting techniques mainly stiffness enhancement proved effective in reducing target displacements and improving performance classification. The findings emphasize the impact of structural configuration and highlight the role of performance-based seismic design in enhancing the resilience of high-rise buildings.

1. Introduction

In recent decades, the height of high-rise buildings has introduced new challenges in structural engineering, particularly in ensuring stability against lateral loads such as wind and seismic forces. Among the various systems developed to resist such loads, tubular structural systems have proven to be among the most effective for tall buildings due to their superior lateral stiffness and structural

[1] hebasalem57@gmail.com - MSc Candidate, Dept. of Structural Engineering, Zagazig University, Egypt
[2] habdelkader@zu.edu.eg - professor, Dept. of Structural Engineering, Zagazig University, Egypt
[3] abdelbaky1962@gmail.com - Assist., professor, Dept. of Structural Engineering, Zagazig University, Egypt
[4] wadid.william@gmail.com - Assist., Dept. of Structural Engineering, Zagazig University, Egypt

https://doi.org/10.21608/jesaun.2025.403714.1619

efficiency. Introduced in the earl y 1960s by Fazlur Rahman Khan widely recognized as the "father of tubular design" these systems have become a cornerstone of modern high-rise construction [1]. Tubular systems function as hollow vertical cantilevers anchored to the ground, resisting lateral forces through the interaction of perimeter columns and horizontal spandrel beams. Common types of tubular systems include framed tubes, braced tubes, bundled tubes, and TiT systems.as shown in fig.1. In their simplest form, these systems consist of closely spaced exterior columns connected by rigid beams through moment-resisting joints, forming a stiff, integrated structural frame.

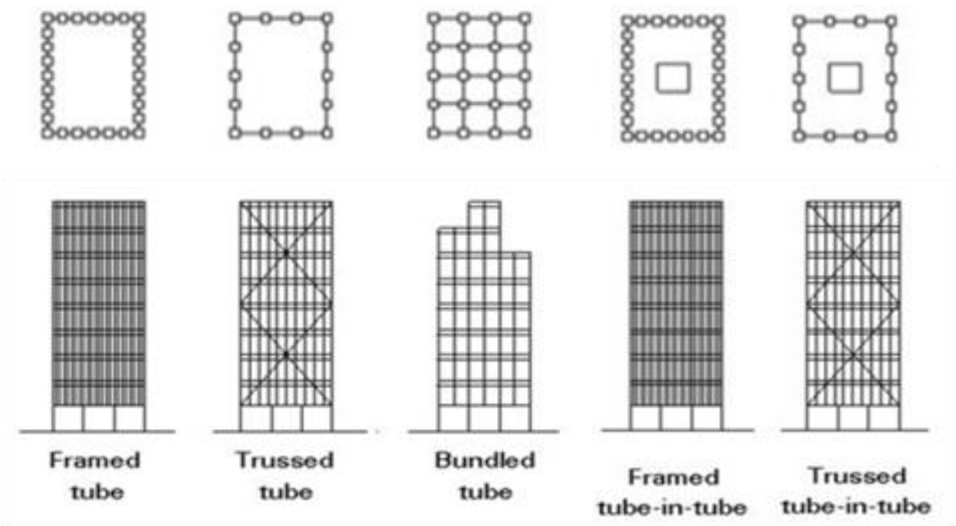

Fig. 1: Diversification of Tubular Structures [1].

One of the most effective configurations, especially for seismic zones, is the tube-in-tube (TiT) system, which combines an outer perimeter frame with an inner reinforced concrete core as shown in fig.2. This dual mechanism enhances seismic performance by efficiently distributing lateral forces across the structure. As recent earthquakes have demonstrated the vulnerability of many high-rise buildings, especially under inelastic deformations, the need for nonlinear seismic evaluation methods has become critical.

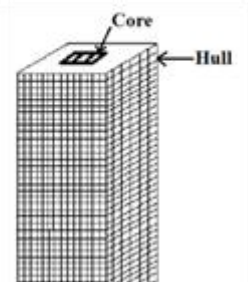

Fig. 2: Tube in Tube system [1]

In this context, pushover analysis has emerged as a practical tool for assessing performance under seismic loading. Two widely adopted frameworks, the Displacement Coefficient Method (DCM) outlined in FEMA-356 [2], and the Capacity Spectrum Method (CSM) from ATC-40 [3] enable engineers to evaluate expected damage patterns and guide retrofitting strategies. This study focuses on evaluating the seismic behavior of reinforced concrete TiT systems with varying heights and configurations, offering insights that support the development of resilient high-rise structures.

2. Literature Review

The seismic performance of high-rise buildings has been the subject of extensive research for several decades, particularly regarding lateral load-resisting systems. One of the earliest and most influential contributions came from Fazlur Rahman Khan in the 1960s, who introduced the concept of tubular structures as an efficient solution for resisting wind and seismic loads. His TiT system, composed of an external perimeter frame and an internal reinforced concrete core, became foundational in the design of modern high-rise buildings due to its structural efficiency and lateral stiffness.

Advancing this concept, the Applied Technology Council (ATC) introduced the Capacity Spectrum Method (CSM) in 1996 as a nonlinear static analysis approach that evaluates structural capacity against seismic demand through performance curves. This was followed by FEMA-356, which developed the Displacement Coefficient Method (DCM). Unlike traditional linear methods, DCM allows for more accurate estimation of inelastic displacement demands, especially in structures expected to undergo significant nonlinear behavior during strong earthquakes. Both methods support the use of pushover analysis as a practical tool to assess structural vulnerability and performance.

Depending on these foundations, Ghasemi (2016) [4] highlighted that vertical and plan irregularities in TiT buildings significantly increase inter-story drifts and induce concentration of plastic hinges, particularly in taller structures. His findings support the view that regular configurations provide better lateral stiffness, improved energy dissipation, and more favorable performance under seismic demands.

Kamal, Inel, Cayci (2022) [5] examined the seismic behavior of mid-rise adjacent RC buildings considering soil–structure interaction. They concluded that flexible soil conditions amplify inter-story drifts and pounding potential, emphasizing the need for foundation–superstructure interaction modeling in performance evaluations.

Bashandy et al. (2021) [6] investigated the effect of vertical irregularities such as building setbacks on seismic response. Their analysis showed that these irregularities disturb force distribution, causing early hinge formation and uneven stiffness degradation. This highlights the importance of accounting for vertical discontinuities in design.

To et al. (2022) [7] performed a comparative seismic analysis using ETABS on framed, framed tube, and TiT buildings. They found that TiT systems offered superior control of lateral displacement, especially in high-rise and high-seismic zone applications, supporting their effectiveness in real-world scenarios.

Kim et al. (2020) [8] analyzed the effect of varying the core-to-perimeter stiffness ratio in TiT structures. Their findings revealed that increasing the stiffness of the core improves energy dissipation and drift control. However, they cautioned that excessive stiffness may result in stress concentrations in the outer frame, leading to premature structural damage.

Oz, Abdel Raheem, Turan (2025) [9] investigated the use of tuned mass dampers to mitigate the adverse effects of torsional irregularity in L-shaped RC structures while accounting for soil–structure interaction. Their results showed that optimally tuned dampers significantly reduced torsional responses, peak drifts, and base shear demands, offering an effective retrofitting strategy for irregular plan configurations.

Atmaca et al. (2024) [10] combined field observations and numerical simulations to assess seismic damage in RC and masonry minarets following the February 6th, 2023, Kahramanmaraş earthquakes (Mw 7.7 and Mw 7.6) in Turkiye. Their findings highlighted critical vulnerabilities in slender vertical structures, particularly at geometric transitions, and stressed the importance of detailing and material continuity for seismic resilience.

Lu et al. (2025) [11] introduced a resilience-based evaluation framework for frame-core tube structures. Their work, based on nonlinear time-history analysis using SeismoStruct, integrated performance loss indices and post-earthquake reparability into the assessment process. This holistic approach is particularly relevant to reinforced concrete TiT systems seeking long-term seismic resilience.

In summary, the literature reveals that while TiT configurations are highly effective in resisting seismic forces, detailed nonlinear analyses particularly using DCM and CSM are essential to accurately capture their behavior. These methods provide critical insights for performance-based seismic design and retrofitting decisions. The present study builds upon this body of work by applying pushover analysis using SeismoStruct software [12] to assess the seismic behavior of reinforced concrete TiT high-rise buildings, considering both regular and irregular configurations across varying building heights and seismic zones.

3. Objectives

This paper aims to evaluate the seismic performance of R.C TiT structures using nonlinear static pushover analysis based on ATC-40 guidelines. The study focuses on three building heights (G+29), (G+39) and (G+49) stories, located in variable intensity seismic zones according to Egyptian Code (ECP-201) [13],; low intensity zone 2 with ag = 0.125g; medium intensity zone 4 with ag = 0.2g and high intensity zone 5b with ag = 0.3g to determine the need for retrofitting, The main objectives are as follow:

- Evaluate the influence of height, seismic zone, and structural regularity on seismic behavior.
- Identify failure mechanisms in critical members and propose suitable retrofitting techniques.
- Simulate the evaluation before and after retrofitting using SeismoStruct software.
- Assess the effectiveness of retrofitting in improving structural performance and reducing target displacement.

4. Nonlinear Static Procedure

The nonlinear static procedure also known as pushover analysis, consists of a series of sequential elastic analyses, superimposed to approximate a force-displacement curve of the overall structure. A two- or three-dimensional model which includes bilinear or trilinear load-deformation diagrams of all lateral force resisting elements is first created and gravity loads are applied initially and held constant. A predefined lateral load pattern which is distributed along the building height is then applied. The lateral forces are increased until some member's yield. The structural model is modified to account for the reduced stiffness of yielded members and lateral forces are again increased until additional members' yield. The process is continued until a control displacement at the top of building reaches a certain level of deformation or structure becomes unstable, in this method the weak spots in the structure can be predicted by what is called plastic hinges. The roof displacement is plotted with base shear to get the global capacity curve fig.3.

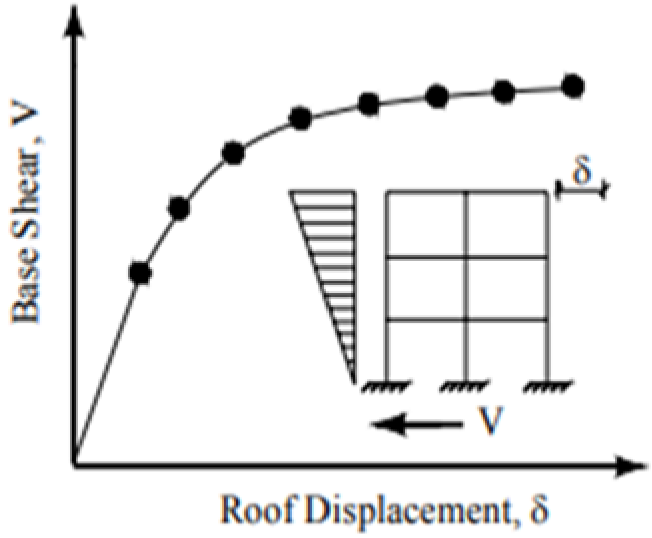

Fig. 3: Global Capacity Curve [3]

5. Seismic evaluation criteria

The seismic evaluation according to ATC-40 can be categorized into two groups: (1) global/structural limits and (2) local/ component limits [3]. The global limits are the ability to sustain gravity load, lateral load, and lateral deformation. If the ability to sustain gravity load is lost by a component, the building must be able to redistribute the load to other components. The structure system's lateral load resistance does not degrade by more than 20% of the structure's maximum resistance. The lateral deformation of the buildings must be tested against the deformation limits as shown in Table 1. The maximum lateral deformation or the maximum drift is known as the inter-story drift at the target displacement, which is calculated according to eq.1.

$$\delta_t = C_0 \times C_1 \times C_2 \times C_3 \times S_a \times T_e^{\,2} \times g \backslash 4\pi^2 \quad (1)$$

Where: δ_t Is known as target displacement or performance point of the building.
C_0, C_1, C_2, C_3 are modification factors calculated according to ATC-40 [3]
S_a = Response spectrum acceleration, at the effective fundamental period T_e of the building.
The inter-storey drift ratio (IDR) is computed from the performance-point displacement profile as the ratio of relative displacement between successive stories to the story height eq.2.

$$\text{IDR} = \frac{\Delta_i - \Delta_{i-1}}{h_i} \quad (2)$$

Where Δ_i and Δ_{i-1} are the total lateral drifts of the two successive floors and hi is the floor height between the two successive floors.
The local/component limits are the element checks. It must be done for all the components of each floor. The deformation capacity of beams and columns controlled by flexure is defined in terms of the total chord rotation capacity; θ as specified in eq.3. The acceptance criteria for plastic hinge

rotations of beam and column elements in the RC moment-resistant frame are presented in Tables ٢ and Table ٣, respectively, as indicated by ATC-40. Therefore, it should be ensured that a member's flexural demand failure and shear failure do not occur before these limits of rotation are reached.

$$\theta = \theta y + \theta p \quad (3)$$

Where: **θ_y: The chord rotation capacity at yield, θ_p; The plastic part of the chord rotation capacity**

Table 1. Lateral deformation limits according to ATC-40 [3]

Story drift limit	Story drift ratio after analysis	Performance Level			
		Intermediate Occupancy	Damage Control	Life Safety	Structural Stability
Maximum Total Drift	0.0039	0.01	0.01-0.02	0.02	$0.33\ S_i\,/\,W_i$ $(0.021)_{at\ roof}$

Table 2. Acceptance Criteria for columns controlled by flexure according to ATC-40 [3]

Conditions			Modeling Parameters[4]			Acceptance Criteria[4]				
			Plastic Rotation Angle, radian		Residual Strength Ratio	Plastic Rotation Angle, radian — Performance Level — Component Type				
						IO	Primary		Secondary	
			a	b	c		LS	CP	LS	CP
i. *Columns controlled by flexure*[1]										
$\frac{P}{A_g f'_c}$	Trans. Reinf.	$\frac{V}{b_w d\sqrt{f'_c}}$								
≤ 0.1	C	≤ 3	0.02	0.03	0.2	0.005	0.015	0.02	0.02	0.03
≤ 0.1	C	≥ 6	0.016	0.024	0.2	0.005	0.012	0.016	0.016	0.024
≥ 0.4	C	≤ 3	0.015	0.025	0.2	0.003	0.012	0.015	0.018	0.025
≥ 0.4	C	≥ 6	0.012	0.02	0.2	0.003	0.01	0.012	0.013	0.02

Table 3. Acceptance Criteria for beams controlled by flexure according to ATC-40 [٣]

Conditions			Modeling Parameters[3]			Acceptance Criteria[3]				
			Plastic Rotation Angle, radian		Residual Strength Ratio	Plastic Rotation Angle, radian — Performance Level — Component Type				
						IO	Primary		Secondary	
			a	b	c		LS	CP	LS	CP
i. Beams controlled by flexure[1]										
$\frac{\rho - \rho'}{\rho_{bal}}$	Trans. Reinf.[2]	$\frac{V}{b_w d\sqrt{f'_c}}$								
≤ 0.0	C	≤ 3	0.025	0.05	0.2	.010	0.02	0.025	0.02	0.05
≤ 0.0	C	≥ 6	0.02	0.04	0.2	0.005	0.01	0.02	0.02	0.04
≥ 0.5	C	≤ 3	0.02	0.03	0.2	0.005	0.01	0.02	0.02	0.03
≥ 0.5	C	≥ 6	0.015	0.02	0.2	0.005	0.005	0.015	0.015	0.02

6. Model Geometry

In this study, the structure is R.C structure. Both regular and irregular TiT structures consist of six bays in the X and Y directions, as shown in Fig.4. Three structure heights are considered to represent high-rise structures: (G+29), (G+39) and (G+49) stories, with a uniform story height of 3٠٠٠.0 mm, as shown in fig.4. These variations aim to capture the seismic performance of TiT systems across different building heights and structural configurations.

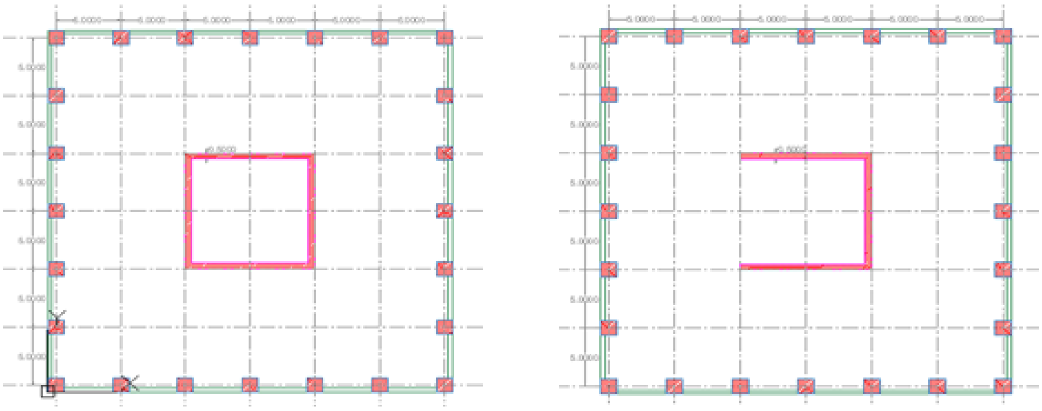

Regular Structure Irregular Structure

Fig. 4: Plan geometry of studied Structure.

The exterior structural system consists of perimeter columns with a constant cross-sectional dimension of 1200 mm × 1200 mm, forming the outer tube of the structure. These columns are interconnected by deep beams in both X and Y directions, each having a cross section of 300 mm × 1000 mm, creating a rigid perimeter frame that enhances lateral stiffness. Internally, the structure includes a central reinforced concrete core wall 500 mm thick, which extends continuously over the full building height, acting as the inner tube. The floor system is composed of flat slabs with a uniform thickness of 300 mm. The geometric and reinforcement details of all structural elements are provided in Table 4.

Table 4. Properties of building members

Element	Height (mm)	Width (mm)	Cover (mm)	Long. Reinf.	Trans. Reinf.
Col	1200	1200	25	32 Ø 25	Ø10/150mm
beam	1000	300	25	5 Ø18 (lower) 5Ø 18 (upper)	Ø10/150mm

To evaluate their behavior under seismic loading, the studied models are arranged in groups to assess the influence of the number of stories as presented in Table ٥. Each group is arranged to assess different seismic zones. All models are developed and analyzed using SeismoStruct software, which allows for nonlinear static (pushover) analysis and detailed evaluation of post-elastic performance.

Table 5. Studied model's parameters

Group	ID	Seismic Zone	Regular/Irregular
(1) (G+29) Stories	BN30Z2R	2	R
	BN30Z4R	4	R
	BN30Z5BR	5b	R
	BN30Z2IR	2	IR
	BN30Z4IR	4	IR
	BN30Z5BIR	5b	IR
	BN40Z2R	2	R

Group	ID	Seismic Zone	Regular/Irregular
(2) (G+39) Stories	BN40Z4R	4	R
	BN40Z5BR	5b	R
	BN40Z2IR	2	IR
	BN40Z4IR	4	IR
	BN40Z5BIR	5b	IR
(3) (G+49) Stories	BN50Z2R	2	R
	BN50Z4R	4	R
	BN50Z5BR	5b	R
	BN50Z2IR	2	IR
	BN50Z4IR	4	IR
	BN50Z5BIR	5b	IR

7. SeismoStruct Software

Seismostruct Software program is a finite element program, which considers both geometric nonlinearities and material inelasticity. It can also predict, under static or dynamic loading, the large displacement behavior of space frames. The three-dimensional modelling is carried out as shown in Fig.5.

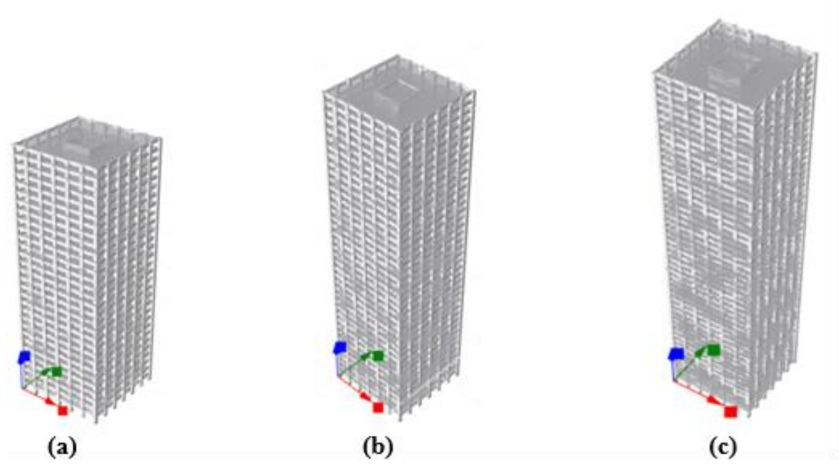

Fig.5: (a) (G+29) story structure; (b) (G+39) story structure; (c) (G+49) story structure.

7.1. Material properties

The concrete modeled as (Mander et al. nonlinear concrete model - con_ma) [14]; C40/50 with Confinement factor =1.2, and the reinforcement steel is modeled as (Menegotto-Pint steel model) [15]; S420 with parameters shown in Table 6. The soil type is classified as Type C, based on the Egyptian Code for Loads (ECP-201), which reflects medium-dense soil.

Table 6. Materials Properties

Concrete Properties; C40/50	
compressive strength; fc (MPa)	40.0
Modulus of elasticity; Ec (MPa)	32563.0

Strain at peak stress; $\boldsymbol{\varepsilon c}$	0.002
Specific weight; $\boldsymbol{\gamma}$ $(kN/m3)$	24.00
Reinforcement properties; S420	
Modulus of elasticity; $\boldsymbol{Es}$ (GPa)	200.0
Yield strength; $\boldsymbol{fy}$ (MPa)	420.0
Strain hardening parameter; $\boldsymbol{\mu}$ (-)	0.005
Fracture/buckling strain; $\boldsymbol{\varepsilon ult}$ (-)	0.10
Specific weight; $\boldsymbol{\gamma}$ $(kN/m3)$	78.0

7.2. Sections Properties

Beams and columns are modeled as 3D inelastic plastic hinge force-based frame element elements (infrmFBPH) with concentrated inelasticity within a fixed length, where the plastic hinge is concentrated at the ends of element. The length of plastic hinge was calculated using eq.4, which was suggested by Scott and Fenves [16].

$$\boldsymbol{L_p} = \mathbf{0.08}\boldsymbol{L} + \mathbf{0.022}\boldsymbol{f_y d_b} \qquad (kN\ ,\ mm) \tag{4}$$

Where, L $=$ length of the member; and fy and db are yield strength and diameter, respectively, of the longitudinal reinforcing bars. The advantage of this approach is that the plastic hinge length includes the effect of strain softening and localization as determined by experiments.

The number of triangular meshes used in section equilibrium computations is set to be 150 and 200 for cross-sections of beams and columns respectively as shown in Fig.6. The floor slab of the building possessed very high in-plane stiffness compared to the out-of-plane one; therefore, these elements are modeled as "rigid diaphragm".

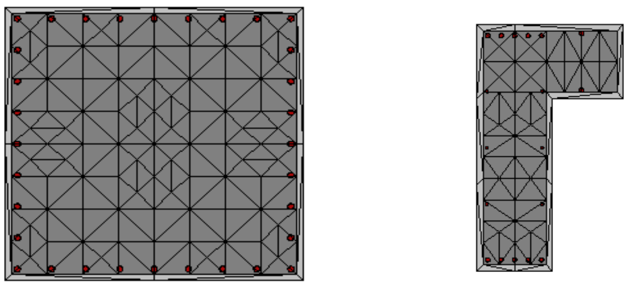

(a) **(b)**

Fig. 6: section discretization (triangular meshes); (a) columns; (b) Beams.

7.3. Loads

- **Gravity loads**

  The loads introduced in the software Seismostruct are the dead loads (G) and live loads (Q). Snow loads are very small where the building is located, and they are neglected. The dead loads include the self-weight of the members and finishing loads (G’). The live loads of the slabs are 5.0 KN/m² applied uniformly across all floor slabs.

- **Lateral loads**

  According to the Egyptian code of loading; (ECP 201), The seismic load or base shear force is calculated and the seismic performance is assessed using pushover analysis as outlined in ATC-

40 and FEMA-365, distributed using a triangular load pattern. Then the models are pushed in 100 steps until target displacements are reached or until failure happens. The displacement is measured by the software using a control node that is located in the center of mass of the roof floor.

8. Results and Discussion

Fig.7 illustrates the pushover curves for the studied TiT structural models with varying numbers of stories. These curves represent the global lateral load displacement behavior of the structures, reflecting their overall stiffness and ductility. By increasing the number of stories, the slope of pushover curves is gradually reduced. This is because of the progressive development of plastic hinges in the beam and column under lateral loading.

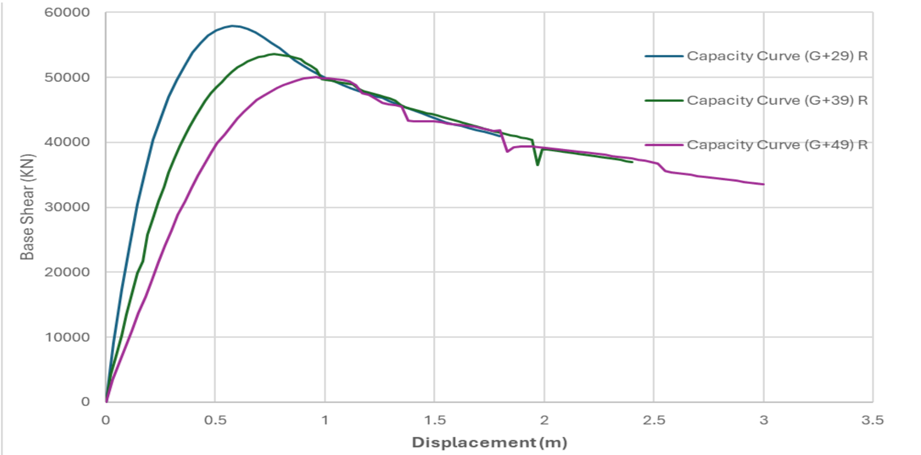

(a) Regular structures.

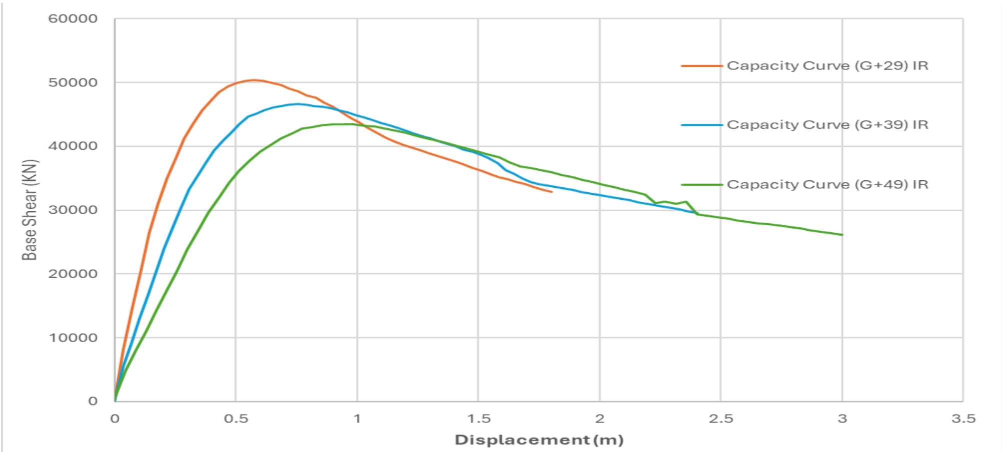

(b) Irregular structures.

Fig. 7: pushover curve for different stories structures (a) Regular structures; (b) Irregular structures.

Figure 8. Shows the pushover curve with the performance point for each structure in different seismic zones according to ATC-40 calculation; as shown in these figures for the same story structure; with increasing the seismicity action the performance point of the structure increase with the same capacity curve.

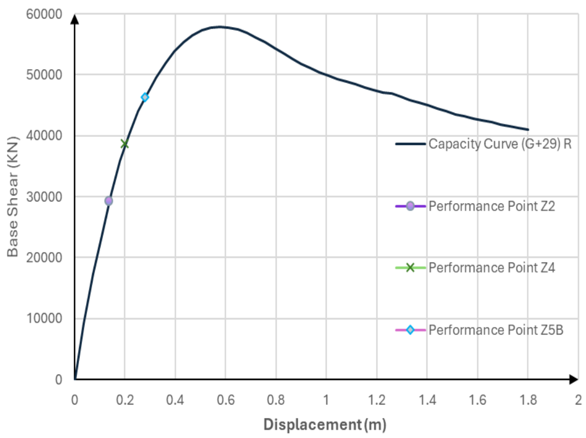

(a) (G+29) R story

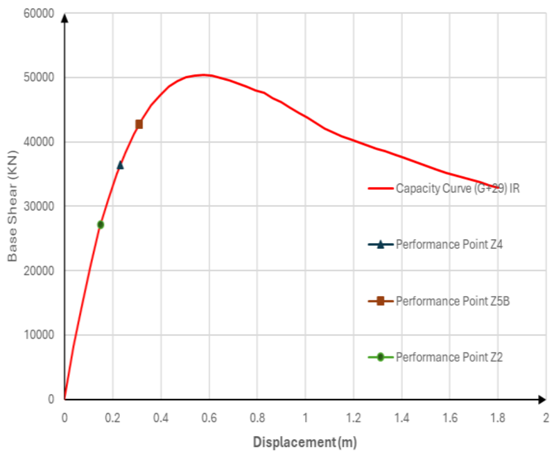

(a) (G+29) IR story

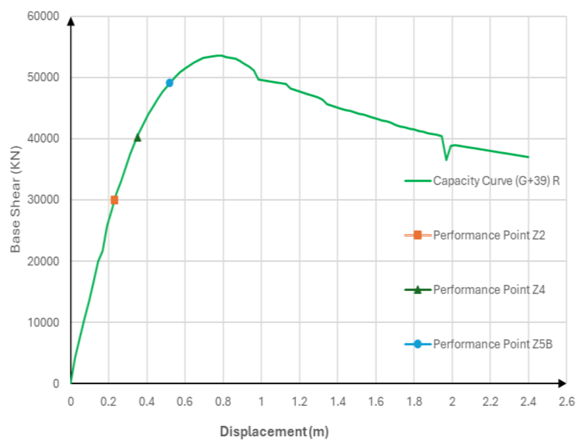

(b) (G+39) R story

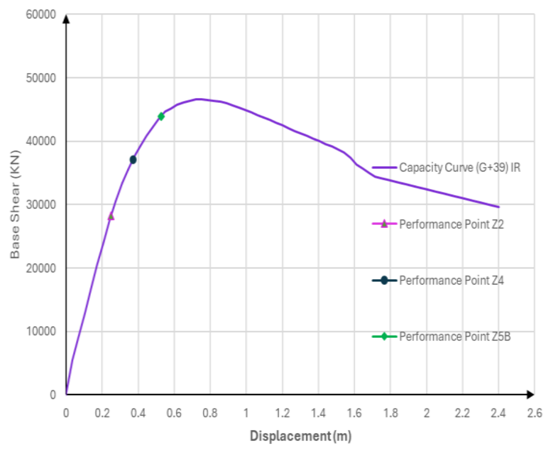

(b) (G+39) IR story

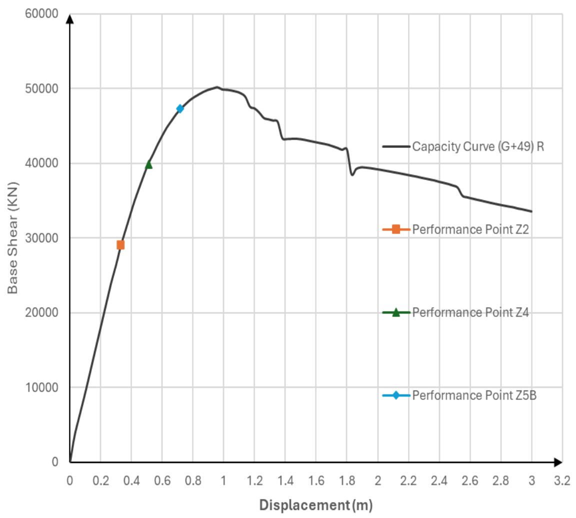

(c) (G+49) R story

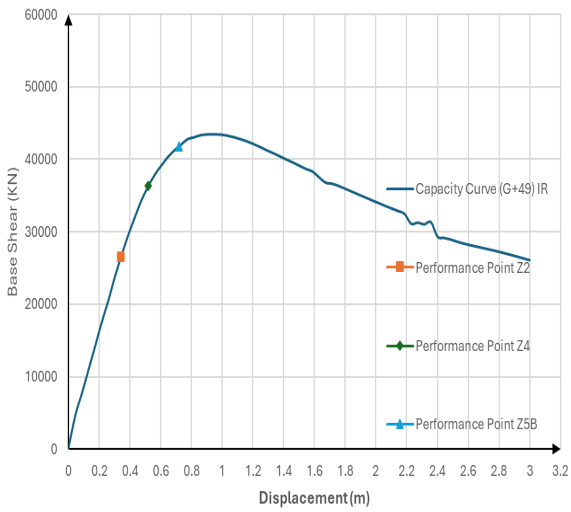

(c) (G+49) IR story

Fig. 8. Pushover curve with performance point for: (a)) G+29)story structure; (b)) G+39)story structure; (c)) G+49)story structure; located in different seismic zones.

Figure 9a. Shows the inter-story drift ratios for the models with (G+29) story at the calculated performance points. This figure showed that; the maximum inter-story drift ratio was located at seventeen with 0.18%, the seventeen with 0.26% and sixteen with 0.36% for structure located in seismic zone 2, 4 and 5b, respectively. The maximum inter-story drift ratio for Irregular models was located at fourteen 0.21%, thirteen with 0.31% and thirteen with 0.41% for structure located in seismic zone 2, 4 and 5b, respectively. The maximum story drifts for all buildings are < 1.0%, which can be categorized in immediate occupancy (IO) performance level as specified in Table 1.

Figure 9.b. shows the inter-story drift ratios for the models with (G+39) story at the calculated performance points. For regular models, the maximum inter-story drift ratio was located at the twenty-one with 0.23%, the twenty with 0.35% and nineteen with 0.51% for structure located in seismic zone 2, 4 and 5b, respectively. The maximum inter-story drift ratio for Irregular models was located at seventeen 0.26%, seventeen with 0.38% and sixteen with 0.55% for structure located in seismic zones 2, 4 and 5b, respectively. The maximum story drifts for all buildings are < 1.0 %, which can be categorized in immediate occupancy (IO) performance level as specified in Table 1.

Figure 9.c. shows the inter-story drift ratios for the models with (G+49) story at the calculated performance points. For regular models, the maximum inter-story drift ratio was located at the twenty-five with 0.27%, the twenty-four with 0.41% and twenty-three with 0.57% for structure located in seismic zone 2, 4 and 5b, respectively. The maximum inter-story drift ratio for Irregular models was located at twenty-one 0.29%, twenty with 0.44% and nineteen with 0.62% for structure located in seismic zone 2, 4 and 5b, respectively. The maximum story drifts for all buildings are < 1.0%, which can be categorized in immediate occupancy (IO) performance level as specified in Table 1. Conclusion, the maximum IDR for regular ranges from (0.18-0.57) % while the maximum IDR for irregular ranges from (0.21-0.62) %. Generally, it is observed that the maximum inter-story drift ratio for irregular models is higher than regular by about 11%.

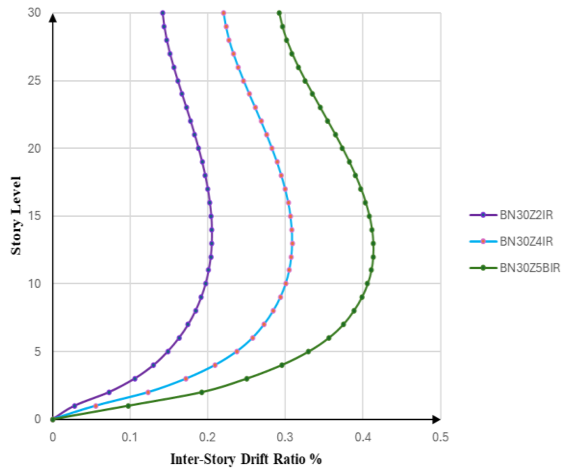

(a) (G+29) R story

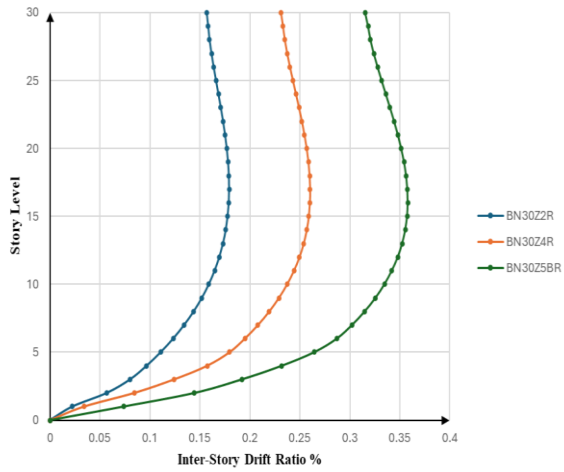

(a) (G+29) IR story

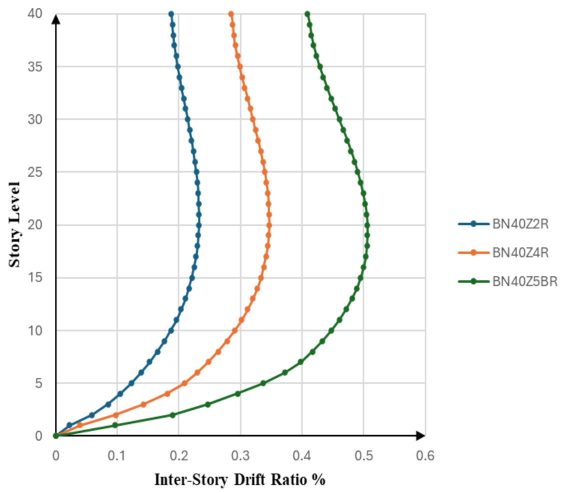

(b) (G+39) R story

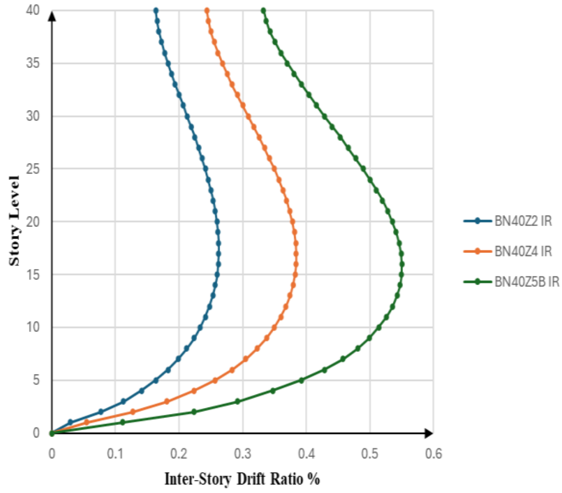

(b) (G+39) IR story

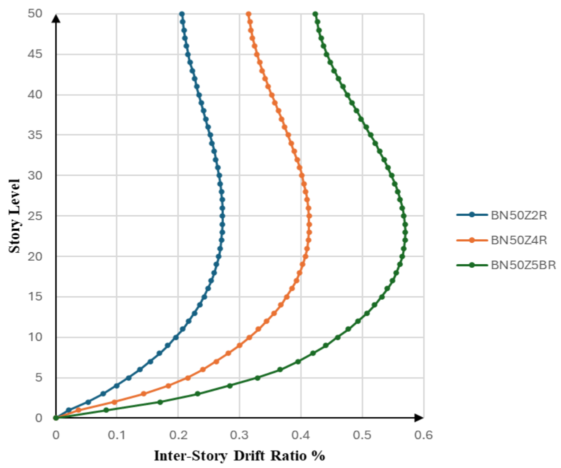

(c) (G+49) R story

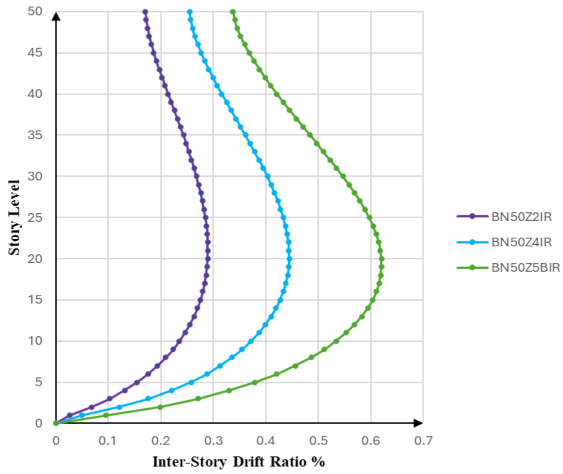

(c) (G+49) IR story

Fig. 9. The inter-story drift ratios at performance points: for; (a) G+29 story structure; (b) G+39 story structure; (c) G+49 story structure; located in different seismic zones

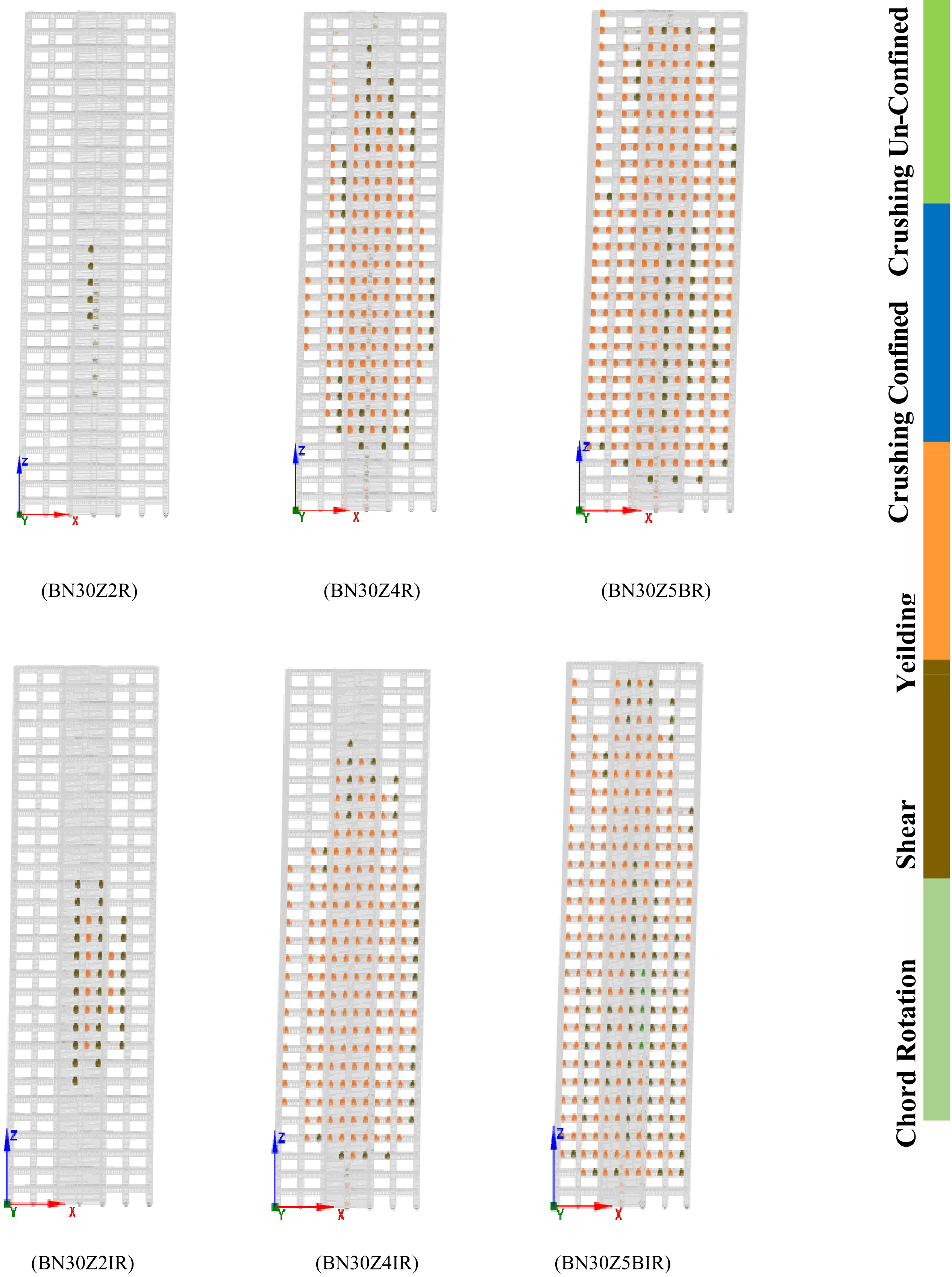

a) (G+29) R/IR story

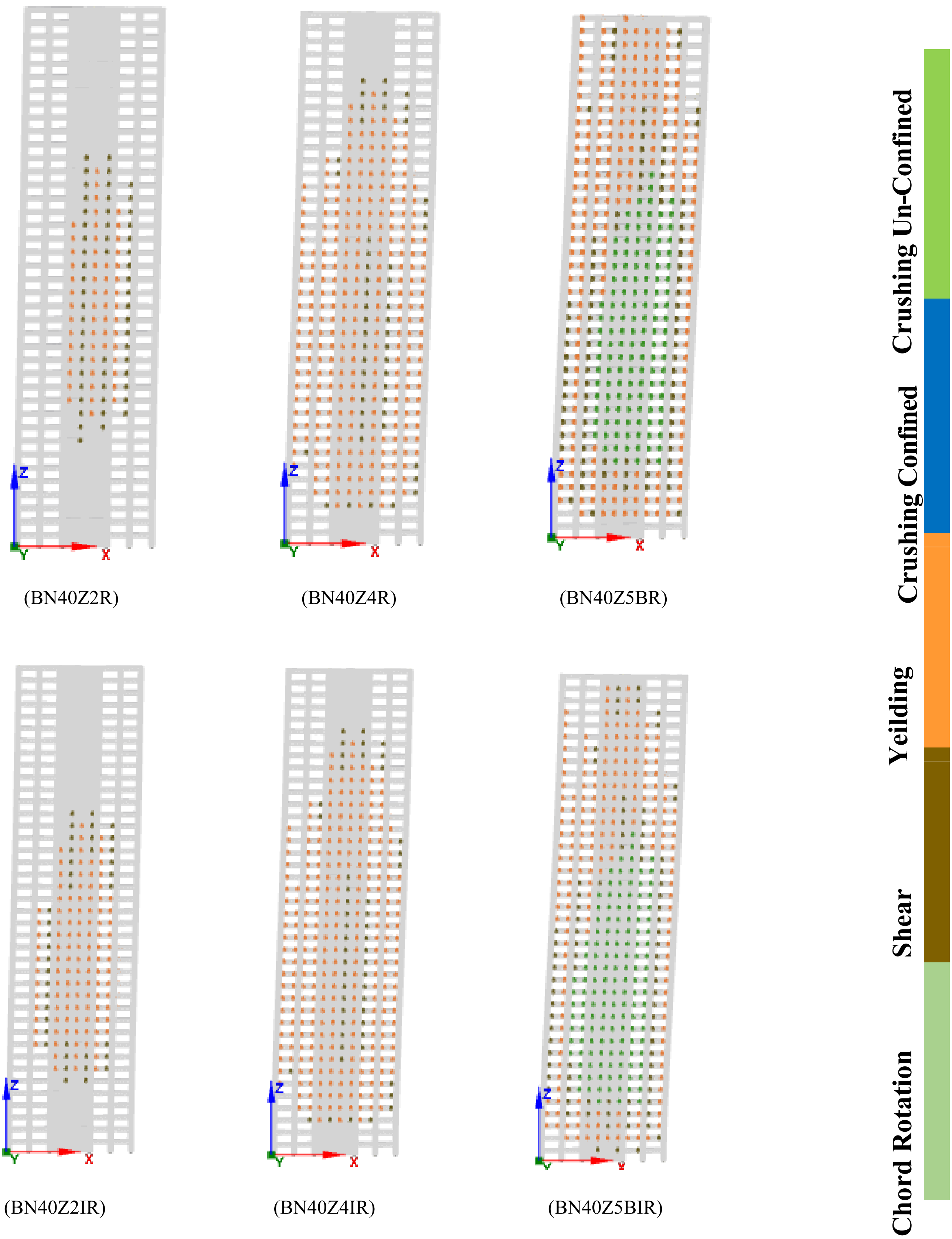

b) (G+39) R/IR story

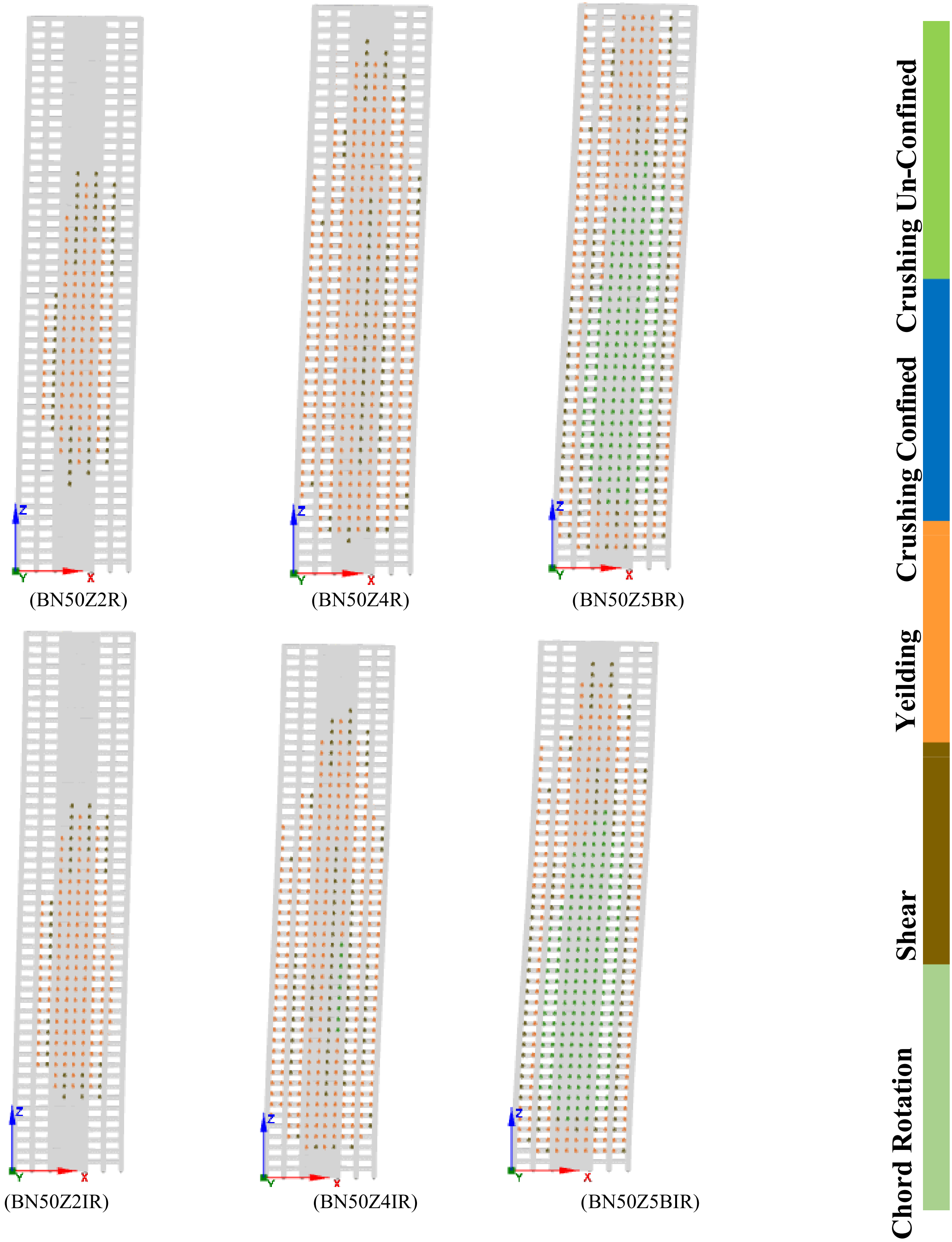

c) (G+49) R/IR story

Fig. 10. Plastic hinge formation at the performance point for; (a) G+29 story structure; (b) G+39 story structure; (c) G+49 story structure; located in different seismic zones.

The deformed shapes and Plastic hinges formation have been gained at various displacement levels or performance points as shown in Fig.10. The sequence of damage of different stories TiT structures is shown in fig.11. As shown in these figures the yielding and shear capacity of some members are reached very early for all structures located in different seismic zones; so, all tube in tube structures needed to be retrofitted.

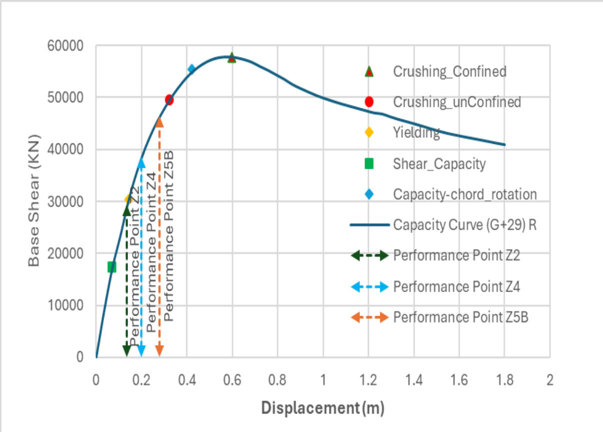

(a) (G+29) R story

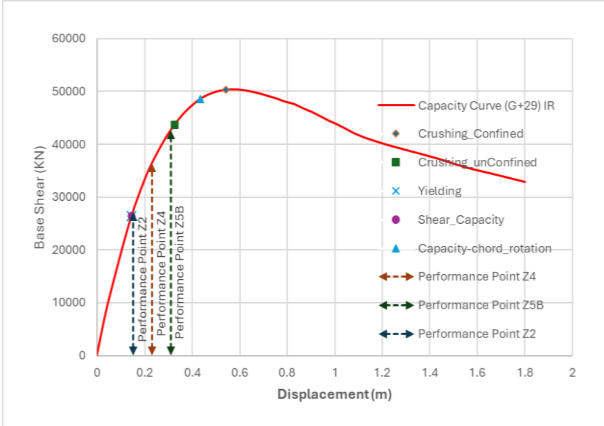

(a) (G+29) IR story

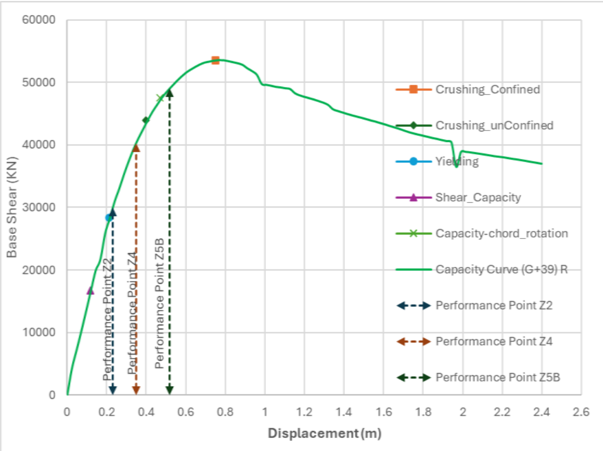

(b) (G+39) R story

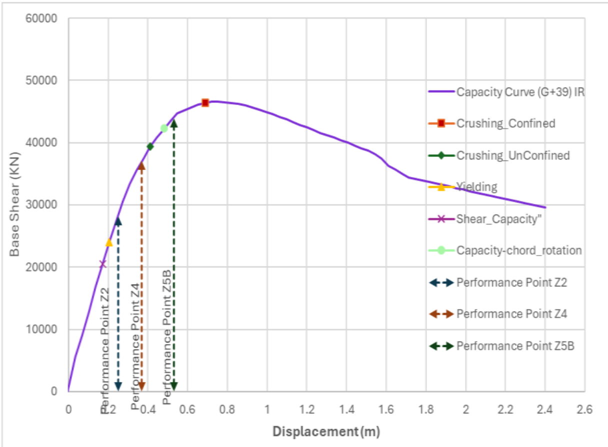

(b) (G+39) IR story

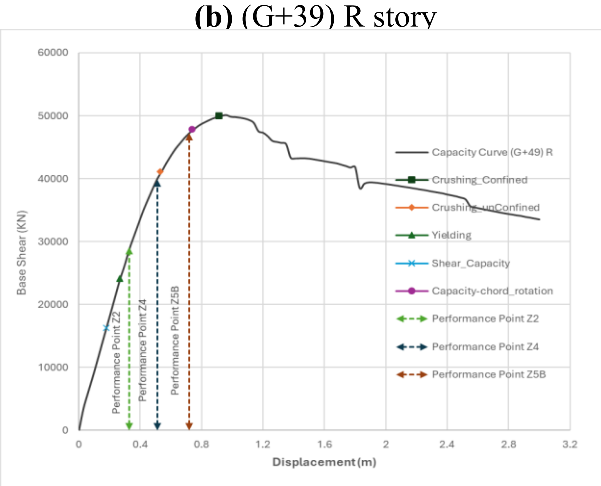

(c) (G+49) R story

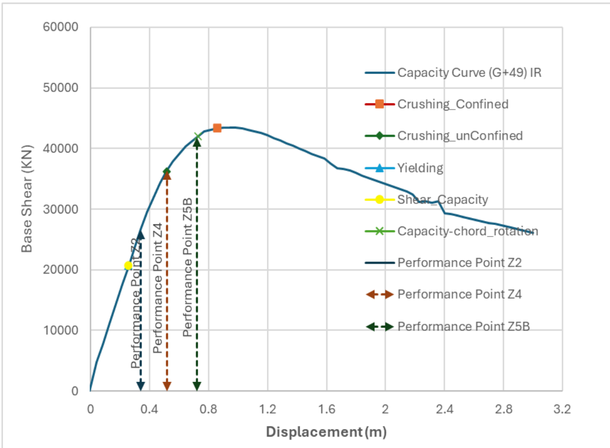

(c) (G+49) IR story

Fig. 11. Sequence of damage: for; (a) G+29 story structure; (b) G+39 story structure; (c) G+49 story structure; located in different seismic zones

Figure 12. Shows the ductility ratio and the over- strength of structures. It was observed that the ductility ratio and the over- strength decreased with increasing number of stories. Tables 7 showed the values of ductility ratio of structures ranged between (2.42 to 1.84), and (2.41 to 1.76) for Regular and Irregular respectively. While the over strength of structures between (1.14 to 1.08) and

(1.14 to 1.08), for regular and Irregular respectively. It was observed that over strength increased when the ductility of the frame increased. On the other hand, with increasing number of stories structures were decreased in ductility and stiffness observe (G+29) and (G+39) structures still in range ductile behavior. While the (G+49) structures had a low ductile ratio and behaved in a brittle manner. According to ATC-40 classification as specified in Table 8, buildings with a ductility ratio below 2 are considered to have low ductility demand, indicating limited deformation capacity under seismic loading. In this study, both (G+49) regular and irregular configurations exhibited ductility ratios of 1.84 and 1.76, respectively. Therefore, it is recommended to evaluate these structures further and consider appropriate retrofitting techniques to enhance their seismic performance and ensure life safety.

Table 7: Ductility and over-strength of

Regular structures

Number of stories	V_{max} (kN)	V_y (kN)	Δ_u(m)	Δ_y (m)	DR	Ω
(G+29) R	57895.09	50694.82	0.576	0.238	2.42	1.14
(G+39) R	53549.506	48050.4	0.768	0.358	2.14	1.11
(G+49) R	50114.17	46223.39	0.96	0.52	1.84	1.08

Irregular structures

Number of stories	V_{max} (kN)	V_y (kN)	Δ_u(m)	Δ_y (m)	DR	Ω
(G+29) IR	50355.335	44121.03	0.576	0.239	2.41	1.14
(G+39) IR	46611.635	41988.72	0.754	0.359	2.10	1.12
(G+49) IR	43340.109	39959.18	0.92	0.50	1.76	1.08

Table8: Component Ductility Demand Classification ATC40 [3].

Max. value for drift ductility	Classification
< 2	Low ductility demand
2 to 4	Moderate ductility demand
> 4	High ductility demand

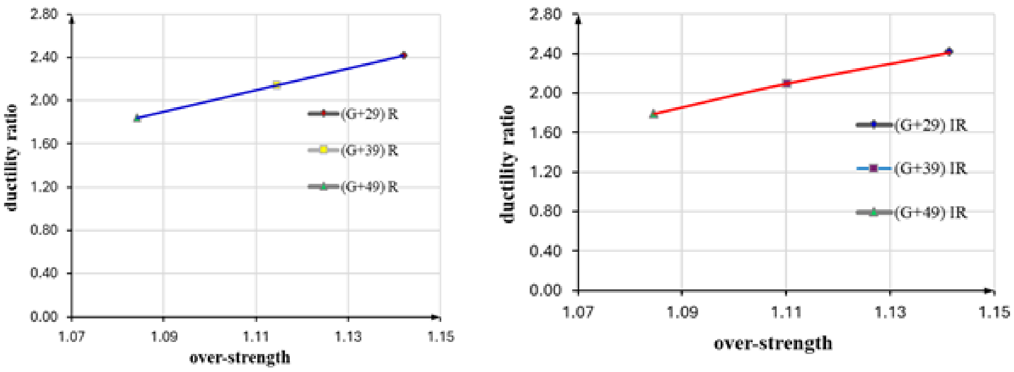

Fig. 12: Over-strength-ductility relationship.

9. Retrofitting Techniques and Modelling Details

After identifying the critical weaknesses in TiT structures using pushover analysis, retrofitting techniques become essential to improve their seismic resilience. Retrofitting can be broadly categorized into local and global techniques, each addressing different structural deficiencies observed in both regular and irregular TiT configurations.

9.1. Global Retrofit Techniques

These techniques enhance the overall structural system, improving global seismic performance. Techniques include:

- Adding shear walls or braced frames.
- Installing outriggers or external dampers.
- Strengthening foundations or core elements.

9.2. Local Retrofit Techniques

These focus on specific vulnerable components such as:

- Concrete jacketing: involves addition of a layer of concrete, longitudinal bars and closely spaced ties. The jacket increases both the flexural strength and shear strength of the column or beam.
- Steel jacketing: of column refers to encasing the column with steel plates and filling the gap with non-shrink grout. The jacket is effective to remedy inadequate shear strength and provide confinement to the column. Different types of steel jacketing.

In this study, selected TiT structure with (G+29) story, located in Seismic Zone 5, were subjected to local retrofitting techniques to evaluate their effectiveness. The focus was placed on concrete jacketing of key structural elements such as columns and beams, aiming to improve overall lateral stiffness, delay plastic hinge formation, and reduce displacement demands. Fig.13. shows the sections for concrete jacketing retrofitted members used in the numerical model.

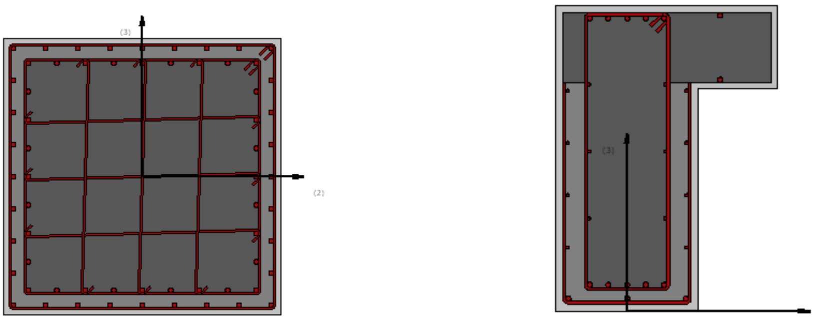

(a) (b)

Fig. 13: section (triangular meshes); (a) columns; (b) Beams.

Fig.14. shows the capacity curves before and after retrofitting for (G+29) story structures. It can be observed that the concrete jacketing retrofitting techniques are improving the performance of the structures by reducing the performance point of (G+29) structure by about 10%.

10. Conclusions

This study aimed to define the performance of structures under seismic loads, based on Pushover analysis. The study introduced has considered three groups of TiT structures located in different seismic zones: The first group (G+29) story, the second group (G+39) story, and the third group (G+49) story to present high rise structures. These structures are designed based on ECP (201). The displacement coefficient method as specified in ATC-40 was used to perform the pushover analysis.

The major conclusions of this study are as follows:

- The TiT system efficiently resists lateral loads through the interaction of a central core and perimeter frame, enhancing overall stiffness and strength in high-rise buildings.
- Pushover analysis is a generally straightforward approach to monitor the nonlinear behavior of the building.
- For the same structure located in different seismic zones; the performance point of the structure increases with increasing seismic zone hazards so the inter-story drift ratio increases as well.
- For the structures with the same stories, the maximum inter-story drift ratio increases with increasing the seismic zone hazard.
- Regular TiT systems generally show uniform distribution of plastic hinges, better stiffness retention, and higher seismic resilience.

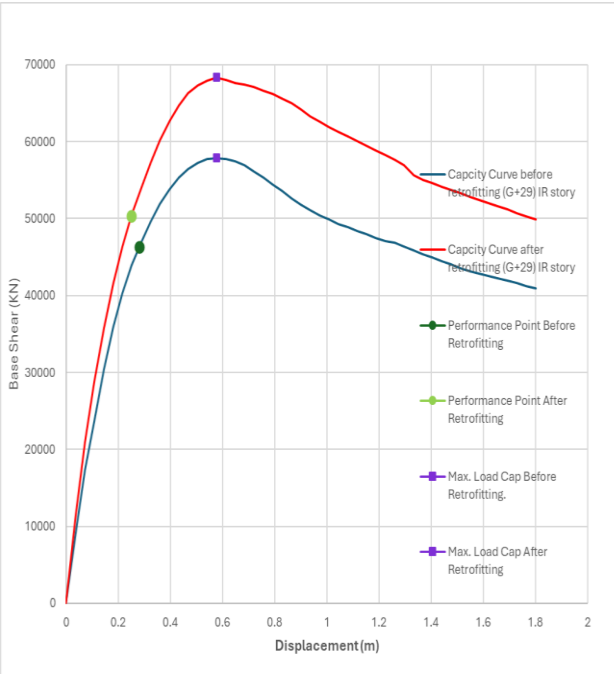

Regular structures.

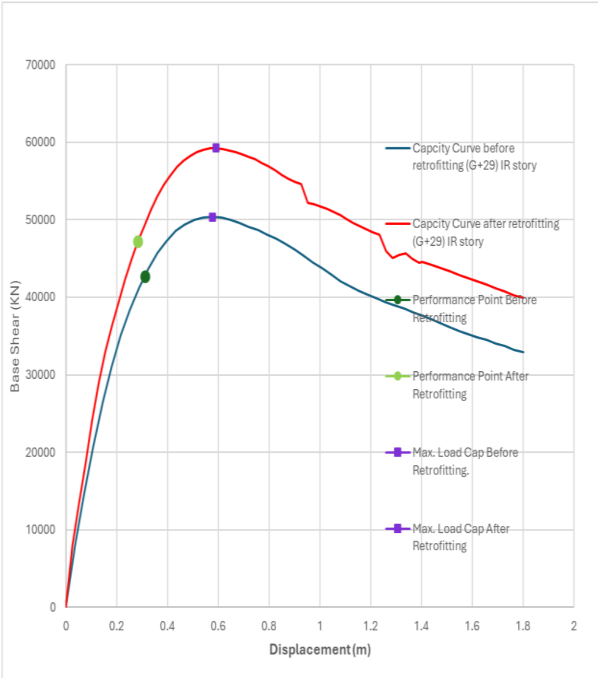

Irregular structures.

Fig. 14: Capacity curves before and after retrofitting for (G+29) story.

- Irregular TiT systems damage tends to concentrate near discontinuities, leading to reduced lateral capacity and earlier loss of ductility compared to regular configurations.
- According to the global/structural limits; which concerned with the lateral deformation; The maximum inter-story drift ratio for all structures located in seismic zones 2, 4 and 5B is expected to be less than 1.0%; this refers to all of these buildings can be classified in Immediate Occupancy (IO) performance level according to ATC-40 specifications.
- According to local/element limits (plastic hinge); it is shown that the yielding and the shear capacity of some members are reached very early for all structures located in different seismic zones; so, all tube in tube structures needed to be retrofitted.
- The global/structural limits are not enough to prove the safety of structures against lateral loads; local/element limits should be carried out too; as shown in this study the global/structural limits showed the safety of all TiT structures to resist lateral loads, but the local/element limits expected that all structures will be a failure and they needed to be retrofitting.

- Implementing retrofitting techniques is critical to enhance structural capacity and performance, particularly for irregular TiT structures, ultimately ensuring they achieve targeted performance.
- Recommendations: Simple, regular structures are safer in earthquakes. If you must use a complex shape, study its effects early, add seismic joints for movement, and keep slabs and connections strong and continuous where the shape changes. Balance stiffness between the core and perimeter and check performance to make behavior more predictable and safer.

References

[1] M. M. Ali and K. S. Moon, "Structural Developments in Tall Buildings: Current Trends and Future Prospects," Architectural Science Review, vol. 50, no. 3, pp. 205–223, 2007.

[2] Federal Emergency Management Agency (FEMA), FEMA-356: Prestandard and Commentary for the Seismic Rehabilitation of Buildings. Washington, DC, USA, 2000.

[3] Applied Technology Council (ATC), ATC-40: Seismic Evaluation and Retrofit of Concrete Buildings, Vols. 1 and 2. Redwood City, CA, USA, 1996.

[4] H. A. Ghasemi, "Evaluation of Seismic Behavior of Irregular Tube Buildings in Tube Systems," Advances in Science and Technology Research Journal, vol. 10, no. 29, pp. 46–51, 2016.

[5] M. Kamal, M. Inel, and B. T. Cayci, "Seismic behavior of mid-rise reinforced concrete adjacent buildings considering soil–structure interaction," Journal of Building Engineering, vol. 51, Art. no. 104296, 2022, doi: 10.1016/j.jobe.2022.104296.

[6] M. Bashandy, A. Elsayed, and H. Abdelrahman, "Effect of Vertical Irregularities on Seismic Performance of High-Rise Buildings," Journal of Building Engineering, vol. 44, Art. no. 102921, 2021.

[7] P. To, N. Lam, and E. Gad, "Comparative Seismic Performance of Tall Building Structural Systems Using ETABS," in Proc. World Conference on Earthquake Engineering, 2022.

[8] Y. J. Kim, H. S. Lee, and J. Y. Cho, "Influence of Core Stiffness on Seismic Response of Tube-in-Tube Buildings," Journal of Structural Engineering (ASCE), vol. 146, no. 2, Art. no. 04019203, 2020.

[9] I. Oz, S. E. Abdel Raheem, and C. Turan, "Mitigation measure using tuned mass dampers for torsional irregularity impact on seismic response of L-shaped RC structures with soil–structure interaction," *Structures*, vol. 79, Art. no. 109449, 2025, doi: 10.1016/j.istruc.2025.109449.

[10] B. Atmaca *et al.*, "Field Observations and Numerical Investigations on Seismic Damage Assessment of RC and Masonry Minarets During the February 6th, 2023, Kahramanmaraş (Mw 7.7 Pazarcık and Mw 7.6 Elbistan) Earthquakes in Türkiye," *International Journal of Architectural Heritage*, early access, Apr. 4, 2024, doi: 10.1080/15583058.2024.2337651.

[11] X. Lu, H. Guan, and P. Pan, "Resilience-Based Seismic Evaluation of Frame-Core Tube Structures Using SeismoStruct," Engineering Structures, vol. 307, Art. no. 115392, 2025.

[12] SeismoSoft, SeismoStruct: A Computer Program for Static and Dynamic Nonlinear Analysis of Framed Structures. Available: https://seismosoft.com.

[13] Research Center for Housing and Building, Egyptian Code for Calculation of Loads and Forces for Buildings (ECP-201). Giza, Egypt, 2012.

[14] J. B. Mander, M. J. N. Priestley, and R. Park, "Theoretical Stress–Strain Model for Confined Concrete," Journal of Structural Engineering (ASCE), vol. 114, no. 8, pp. 1804–1826, 1988.

[15] M. Menegotto and P. E. Pinto, "Method of Analysis for Cyclically Loaded Reinforced Concrete Plane Frames Including Changes in Geometry and Non-Elastic Behavior of Elements," in Proc. IABSE Symposium on Resistance and Ultimate Deformability of Structures Acted on by Well-Defined Loads, Lisbon, Portugal, 1973.

[16] M. H. Scott and G. L. Fenves, "Plastic Hinge Integration Methods for Force-Based Beam-Column Elements," Journal of Structural Engineering (ASCE), vol. 132, no. 2, pp. 244–252, 2006.